SCRAM AND NONLINEAR REACTOR SYSTEM SEISMIC ANALYSIS FOR A LIQUID METAL FAST REACTOR

A. MORRONE

Westinghouse Electric Corporation,
Advanced Reactors Division, Madison, Pennsylvania 15663, U.S.A.

SUMMARY

Earthquake vibrations cause large forces and stresses and can significantly increase the scram time required for safe shutdown of a nuclear reactor. The horizontal deflections of the reactor system components cause impact between the control rods and their guide tubes and ducts. The resulting friction forces delay the travel time of the control rods. To obtain seismic responses of the various reactor system components (for which a linear response spectrum analysis is considered inadequate and to predict the control rod drop time, a nonlinear seismic time history analysis is required. The nonlinearities consist of the clearances or gaps which exist between the various components. When the relative motion of adjacent components is large enough to close the gaps, impact takes place with large impact accelerations and forces. These impact forces are then utilized to calculate scram times.

This paper presents the analysis and results for a liquid metal fast reactor system which was analyzed for both scram times and seismic responses such as bending moments and impact forces. The reactor system was represented with a one-dimensional nonlinear mathematical model with two degrees of freedom per node (translation and rotation). The model was developed to incorporate as many reactor components as possible without exceeding computer limitations. It consists of 12 reactor components with a total of 71 nodes, 69 beam and pin-jointed elements and 27 gap elements. The gap elements were defined by their clearances, impact spring constants and impact damping constants based on a 50% coefficient of restitution. The horizontal excitation input to the model is the response of the containment building at the location of the reactor vessel supports. It consists of a ten seconds Design Basis Earthquake acceleration-time history at 0.005 seconds intervals and with a maximum acceleration of 0.408 g. The analysis was performed with two Westinghouse special purpose computer programs. The first program calculated the seismic responses and stored the impact forces on tape. The impact forces were then input to the second program for the scram time determination.

The results give time history plots of various seismic responses, and plots of scram times as a function of control rod travel distance for the most critical scram initiation times. The total scram time considering the effects of the earthquake was still acceptable but about 4 times longer than that calculated without the earthquake.

1.0 INTRODUCTION

Seismic analyses employing response spectra techniques are usually performed on structural systems which can be adequately modeled with linear elastic dynamic behavior. However, when the system is composed of components which may impact each other due to the clearances among them, a nonlinear time history analysis is required. This type of analysis allows the actual system to be better represented in the model with the proper definition of boundary conditions, and will calculate the various impact forces on the components. A nonlinear seismic time history and a scram analysis which were performed on a liquid metal fast reactor are described in this paper. The description includes the derivation of the mathematical model from the actual system, the calculation of the various input parameters, the scram analysis technique, and typical results. The time history analysis was performed to obtain various seismic responses (such as impact forces and bending moments) for use in other analyses to determine the total effects on the components. The scram analysis was done to calculate the scram times as a function of rod travel distance.

2.0 REACTOR SYSTEM MATHEMATICAL MODEL

The actual reactor system for the development of the analytical model is shown on Fig. 1. Since the scope of the analysis was to determine the responses of selected components such as the reactor vessel and its internals, only those components identified on Fig. 1 were modeled. The resulting mathematical model used in the analysis is shown on Fig. 2. The model is one-dimensional with two degrees of freedom per node (horizontal translation and rotation). Fig. 2 gives a two-dimensional representation for clarification and to show the gaps and springs between the nodes. The inertias and properties used in the model are given in Tables I and II. The lengths of the elements and node locations were optimized to some extent to allow a reasonable value of the integration time constant in the computer solution.

The horizontal seismic excitation is applied at Node 1 and consists of a Design Basis Earthquake (DBE) acceleration-time history at 0.005 seconds intervals developed by the Architect/Engineer at the reactor vessel supports from a finite element analysis of the containment building and foundation system [1]. Only the first ten seconds of the original 20 second time history were input to the computer program since the accelerations after 10 seconds were insignificant. Furthermore, since preliminary analyses with the full 10 seconds showed that the responses from 5 to 10 seconds were small, a total of 5.0 seconds of the earthquake were analyzed.

The reactor vessel head is modeled with a concentrated mass and rotary inertia at Node 1. The head is connected to the containment building (Node 71) through a Z-ring represented by a torsional spring with a spring constant of 6.14×10^{12} in-lb/rad. The reactor vessel is restrained against rotation with a torsional spring between Node 4 and the support on the containment building. The torsional spring constant is 1.67×10^{12} in-lb/rad. which was obtained by combining in series the Z-ring spring constant and that of the vessel support straps of 2.3×10^{12} in-lb/rad. The vessel is connected to the head only in the horizontal translation with a pin joint element between nodes 1 and 3. The masses and rotary inertias of the cylindrical vessel, as well as those of the other uniformly distributed mass components, are calculated internally by the computer program. The sodium mass and the total inertias of the lower head are lumped at nodes 5 and 8. The core support skirt is modeled with an element connecting the vessel and the bottom of the core barrel, and with concentrated mass and rotary inertias of the core support structure. The rotational stiffness of the skirt is represented by a torsional spring with a spring constant of 2.54×10^{11} in-lb/rad. The core barrel is modeled with massless elements but with concentrated masses and rotary inertias at the nodes. These lumped inertias include those of the barrel, sodium, shielding, fuel storage and upper and lower forgings. The remaining components have been modeled as single members. However, their mass and modulus of elasticity have been multiplied by the total number of components which they represent.

3.0 SEISMIC ANALYSIS

3.1 Computer Program

The computer program used for the seismic time history analysis is a special purpose Westinghouse proprietary program, DARI (Dynamic Analysis of Reactor Internals). It is a two-dimensional finite element program which was developed to satisfy the higher efficiency requirement for large nonlinear problems. The program predicts complete time history responses which include displacement, acceleration, velocity, force, moment and shear.

The choice of the integration time constant and the print time interval for the computer solution is very important especially for the high frequency response during impact. The integration time should be only a fraction of the smallest period of any element in the model. The print time should be sufficiently small to obtain the significant response peaks. A value of 25 microseconds for the integration time was determined to be adequately small for good convergence. The print time used in the analysis was 1 millisecond. The adequacy of this value was checked by locating the time region of greatest response and then performing additional "fine tuning runs" in this region with a value of 250 microseconds. The fine tuning runs did not show any significant difference in peak responses.

3.2 Impact Nodes Gaps and Spring Constants

The horizontal clearances of adjacent components which may close and cause impact during the seismic distrubance are shown as single or double impact gaps between nodes. The numerical value of these gaps are given in Table III. DARI uses these gap values in conjunction with the impact spring constant and damping force to calculate the impact force given by

$$F_t = K_t X_r + C_i \dot{X}_r \qquad (1)$$

where:

F_t = nodal impact force;

K_t = nodal impact spring constant;

C_i = nodal impact damping constant;

X_r = penetration distance;

$\dot{X}_r$ = relative velocity of nodes on either side of the gap.

The penetration distance, X_r, is obtained as the difference between the available gap clearance and the relative movement between the nodes on either side of the gap.

The impact spring constants for most of the cylindrical cross-section components were obtained based on Bijlaard's work [2] and considering the impact to occur over a finite area of the cylinder. This considers the local deformation which occurs between two bodies during impact. The resulting spring constants, in this manner, are greater and more realistic than those which would be obtained using an idealized point load. For the components in the core region, which are mostly of hexagonal cross-section, the impact spring constants were based on results of load-deflection data and from previous analyses. From a finite element analysis on a quarter section of a 0.19" thick hexagonal load pad, a spring constant of about 9.4×10^6 lb/in. was obtained. This single duct value was used at the appropriate load pads and multiplied by the thicknesses ratio to the third power for the other load pads of different thickness. For the core barrel, the impact spring constants were calculated with the properties of thick ring forgings at both pad locations.

The above impact spring constants are applicable to a single component. A proportion of series-parallel springs was assumed for the core components, with the aid of the core map, to evaluate an equivalent spring constant. For the fuel assemblies and control rod ducts, a factor of 1.5 was applied to the single component spring constant for an approximate 8 parallel-5 series combination. For the reflectors, with a total of 54 on each side of the model, 18 reflectors were considered to act in parallel and 3 in series, thus giving an 18/3 factor. The resulting values of impact spring constants between adjacent nodes are given in Table III.

3.3 Damping

The damping of the structural system consists of nodal damping and impact damping. The nodal damping forces and moments are proportional to the velocity in both translation and rotation. The nodal damping constants are calculated from,

$$C_t = 2\beta\omega M \tag{2}$$

$$C_r = 2\beta\omega I \tag{3}$$

where:

C_t, C_r = nodal damping constants for translation (lb-sec/ft.) and rotation (lb-sec-ft.), respectively;

β = fraction of critical damping;

ω = component natural frequency in rad/sec;

M = nodal mass, lb-sec^2/ft;

I = nodal rotary inertia, lb-sec^2-ft;

The value of the nodal damping was taken at 2.0% of critical for the DBE in accordance with the criteria given in [3]. The predominant component natural frequencies were obtained from normal mode analysis.

For impact damping, a coefficient of restitution, R_c, of 50% was selected in this analysis to obtain the fraction of critical damping at impact, β_i. This R_c value was considered conservative based on some results of impacting fuel assemblies which showed lower values. The value of β_i for R_c of 0.50 was approximately 0.10. This relationship came from an analytical expression derived at Westinghouse considering the coefficient of restitution as the ratio of the energy input to the energy output, and assuming the deformation at impact to be a damped half-sine wave. The impact damping constants were also calculated with eq. (2) but with the impact frequency, ω_i. For a damped spring-mass system with two masses, m_1 and m_2, representing the nodal masses on each side of the gap, ω_i may be found from [4] as:

$$\omega_i = \left[\frac{(m_1 + m_2)\, K_t}{m_1\, m_2}\right]^{1/2} \tag{4}$$

Substituting eq. (4) in eq. (2) with

$$M = \frac{m_1 m_2}{m_1 + m_2} \qquad (5)$$

yields,

$$C_i = 2\ \beta_i \left[\left(\frac{m_1 m_2}{m_1 + m_2} \right) K_t \right]^{1/2} \qquad \text{or } 2\beta_i K_t / \omega_i \qquad (6)$$

The resulting calculated values of impact damping constants are given in Table III.

3.4 Typical Results

The results of the seismic analysis give time history plots of various responses throughout the model. Fig. 3 shows an example of the responses at the reactor vessel supports. The total seismic force at Node 1 is shown on Fig. 3 (a) and the total seismic moment at Node 71 is shown on Fig. 3 (b). The force equals the sum of the shears in all the elements at Node 1. The moment is equal to $\Sigma K_{\theta i} \theta_i$ where $K_{\theta i}$ is the rocking spring and θ_i is the rotational displacement at node "i", respectively. These relationships are used to perform spot checks of the computer results.

4.0 SCRAM ANALYSIS

4.1 Description

This analysis calculates the control rod motion after the rod has been released from its fully withdrawn position. The time elapsed for the rod to fall to a certain position is called the scram time for that position. The total scram time is the time required for the rod to engage the impact reducing dashpot for a 27 in. of travel. The calculations for scram times consider the impact forces along all the driveline nodes and all other retardation forces on free fall. The equation of downward motion of the control rod is:

$$m\ddot{x} = mg + kx - F_b - F_d - F_{fd} - \mu F_t \qquad (7)$$

where:

m = mass of one control rod, lb-sec^2/in;
$\ddot{x}$ = acceleration of control rod, in/sec^2;
g = gravitational constant, 386 in/sec^2;
kx = scram spring force, lb;
F_b = buoyancy force, lb;
F_d = dashpot force, lb;
F_{fd} = fluid drag force, lb;
μ = coefficient of friction;
F_t = impact force, lb.

Eq. (7) is solved numerically with a special purpose computer program. This program takes the absolute sum of the impact forces at all the driveline impact nodes generated by DARI directly from computer tapes. These are taken at time T_1 for impact force F_1, and at the next time T_2 for F_2. The program interpolates for F_t at time t in the following manner:

$$F_t = [(T_2 - t)/(T_2 - T_1)]\ F_1 + \{1 - [(T_2 - t)/(T_2 - T_1)]\}F_2 \qquad (8)$$

The total friction force at time t, H_t, is obtained by:

$$H_t = F_t\ \mu/N \qquad (9)$$

where N = number of control rods grouped together.

The integration time constant used in the numerical solution of eq. (7) was 50 microseconds. Smaller values did not produce significantly different results. The mass of one control rod, m, was calculated at 0.997 lb-sec^2/in. and the buoyancy force, F_b, at 45.0 lb. A value of 1.0 for the dynamic coefficient of friction was considered to be sufficiently conservative. (The control rod initiated its travel even with a static coefficient of friction of 2.0). The scram spring force, kx, varies linearly from a maximum of 358.4 lb. at zero distance to 12.8 lb. at a travel distance, x, of 14 in. Therefore,

$$kx = 358.4 - 24.686x; \quad (0 \leq x \leq 14) \tag{10}$$

The dashpot force, F_d, acts only when the rod engages the dashpot from a travel distance of 27" to 36". Therefore, it was not used in this analysis. The fluid drag force, F_{fd}, was defined as a function of the control rod velocity by an equation which was verified experimentally.

4.2 Scram Results

A superposition of the impact forces at all the driveline impact nodes is plotted on Fig. 4 for the first 2.5 seconds of the earthquake. This plot serves to indicate the time region of greatest impact disturbance from which various values of scram initiation time are evaluated so that the highest impact forces are considered in the scram analysis. Since nine rods were grouped in the model, the impact forces for a single rod are 1/9 those shown in the plot.

From Fig. 4 it is seen that the impact forces occur after 0.1 seconds. Hence, the scram initiation time was started at 0.1 seconds in the earthquake and varied in increments of 0.1 sec. up to 1.4 seconds. This was done to obtain the worst scram time for both 5 in. and 27 in. of travel. The scram time for the first 5 in. of travel was determined for use in other analyses dealing with reactivity and fuel pin cladding strains. The results are plotted on Fig. 5 which shows the scram time as a function of scram initiation time. For the first 5 in. of rod travel (Fig. 5a) the most critical scram initiation time resulted at 1.3 seconds. For a total of 27 in. of rod travel (Fig. 5b) the worst scram initiation time occurs at 0.4 sec. in the earthquake. Fig. 6 gives the resulting plots of scram time as a function of rod travel distance for the 1.3 sec. and 0.4 sec. scram initiation times. From this figure it is seen that the longest time for the rod to travel the first 5 in. is 0.27 sec., and that for the total of 27 in. of travel is 2.15 seconds. The scram time profile curve for normal operating conditions is also shown on these figures to illustrate the influence of the earthquake disturbance on scram time. This latter curve was obtained with the same scram program by specifying a zero dynamic coefficient of friction.

5.0 CONCLUSIONS

Seismic responses of reactor system components have been obtained from a nonlinear time history analysis considering the actual clearances which exist among the components. Scram times were obtained from a second analysis which used the impact forces generated by the nonlinear analysis. The following results of the analyses show that scram times are significantly increased by friction forces at impact caused by earthquake excitations:

1. Initiating the control rod drop at 1.3 seconds after the start of the earthquake results in a scram time of 0.27 seconds for the first 5 inches of rod travel. The corresponding scram time for normal operating conditions, without the seismic event, is 0.15 seconds.

2. Initiating the control rod drop at 0.4 seconds after the start of the earthquake results in a scram time of 2.15 seconds for the total 27 inches of rod travel to the dashpot. The corresponding scram time for normal operating conditions, without the seismic event, is 0.57 seconds.

Although the scram times are considerably longer with the seismic event than without it, they are still acceptable.

ACKNOWLEDGMENTS

The author wishes to express his appreciation to A. N. Nahavandi for the development of the DARI program and his advice in the analysis, and to W. G. Brussalis for his suggestions and advice.

REFERENCES

[1] Bechtel Corporation, "Supplemental Data for Review of the 2D Seismic Analysis of the Reactor Containment Structure. List of Acceleration Time Histories", B-1763, October 30, 1972.

[2] Bijlaard, P. P., "Stresses from Radial Loads in Cylindrical Pressure Vessels", Welding Research Supplement, December, 1954.

[3] JABE-WADCO-02, "Seismic Design Criteria for the Fast Flux Test Facility", Prepared for Hanford Engineering Development Laboratory, Richland, Washington by J. A. Blume and Associates, Engineers, June, 1973.

[4] Myklestad, N.O., Fundamentals of Vibration Analysis, McGraw-Hill Book Co., Inc., New York, 1956.

TABLE I - CONCENTRATED MASSES AND ROTARY INERTIAS

NODE NO.	MASS (LB-SEC^2/IN)	ROTARY INERTIA (LB-SEC^2-IN)
1	3350.0	1.602×10^7
5	681.7	0
8	630.0	1.578×10^6
9	447.7	1.49×10^6
12	22.5	2.70×10^4
14	49.5	5.90×10^4
26	245.7	4.65×10^5
27	241.3	4.30×10^5
28	217.7	4.06×10^5
29	217.7	4.06×10^5
54	244.0	8.50×10^4
55	12.0	1000.0
56	0.7	13.0
57	1.8	50.0
58	0.8	20.0
59	0.4	10.0

TABLE II - ELEMENT PROPERTIES

ELEMENT NO.	COMPONENT	SIZE O.D. X THK. (IN)	AREA (IN^2)	MOMENT OF INERTIA (IN^4)	DENSITY ($LB-SEC^2/IN^4$) OR * WEIGHT (LB/IN)	EQUIVALENT MODULUS OF ELASTICITY ($LB/IN^2 x10^6$)
1	3-Inst. Tree	23.375 x 1.0	70.3	4400.0	0.0115	69.0
3,4,5,6,7	R. Vessel	247.75 x 2.38	1835.0	13.8×10^6	0.00073	23.5
8	Skirt	230.0 x 2.5	1787.0	11.6×10^6	0.00073	23.5
9	3-I.T.	18.0 x 1.0	53.4	1935.0	0.0022	69.0
10	3-I.T.	18.0 x 1.0	53.4	1935.0	0.0042	69.0
11,12,13	3-I.T.	22.0 x 1.0	66.0	3640.0	0.0046	69.0
14	9-C.R.G	6.4 x 0.38	7.2	32.6	0.0106	207.0
15,16	9-C.R.G	4.76 x 0.76	9.5	19.8	0.0080	207.0
17	9-CRDL	2.19 x 0.25	1.5	0.7	0.0172	207.0
18	9-CRDL	1.88 x 0.188	1.0	0.4	0.0130	207.0
19	9-CRDL	2.40 x 0.125	0.9	0.6	0.0167	207.0
20	9-CRDL	1.12 x 0.56	1.0	0.08	*2.8	232.0
21	9-CRDL	0.5 Solid	0.2	0.003	*0.56	232.0
22,23	9-CRDL	4.09 x 0.026	4.55	0.897	*19.0	232.0
24,25,26	Core B.	144.0 x 2"	892.0	2.25×10^6	0	23.5
27,39	54-Refl.	----	1.467	0.0805	*243.0	1220.0
28,40	54-Refl.	----	4.682	0.0915	*243.0	1220.0
29,41	54-Refl.	----	8.0	30.0	*243.0	1220.0
30,42,31 43,32,44	41-Fuel Assy.	4.575 x 0.120	1.852	5.110	*118.0	927.0
33,34,45,46	4 1/2 C.R.D.	4.575 x 0.120	1.852	5.110	*3.82	102.0
35,47	4 1/2 C.R.D.	4.575 x 0.120	1.852	5.110	*9.79	102.0
53,54	C.I.V.	56.0 x 1.5	256.7	95,400.0	0.00073	26.4
55	9-CRDM N.	7.2 x 0.250	5.6	32.0	0	238.0
56	9-CRDM N.	4.14 x 0.109	1.4	2.8	0	238.0
57	9-CRDM N.	3.44 x 0.250	2.5	3.2	0	238.0
58	9-CRDL	1.49 x 0.157	0.8	0.15	*4.40	232.2
59,60,61	9-CRDL	1.75 x 0.188	0.9	0.29	*4.70	232.2
62	9- CRDL	3.05 x 0.100	0.9	1.0	*8.20	232.2
63	9-CRDL	2.19 x 0.25	1.5	0.73	*7.50	232.2
64,65	9-I.A. CRDM	5.66 x 0.420	6.9	23.8	0.0306	238.0
66	9-I.A. CRDM	5.40 x 0.200	3.3	11.0	0.0288	238.0
67	9-I.A. CRDM	5.40 x 1.75	20.0	41.0	0.0075	238.0
68	9-CRDM N.	7.0 x 0.9	17.2	81.8	0.0067	238.0
69	9-CRDM N.	5.983 x 0.232	4.2	17.3	0.0067	238.0

TABLE III - IMPACT NODE GAPS, SPRING CONSTANTS AND IMPACT DAMPING

BETWEEN NODE NO.	GAP (IN)	IMPACT SPRING CONSTANT ($LB/FT \times 10^6$)	IMPACT DAMPING CONSTANT (LB-SEC/FT)
12 - 18	1.116 (Double)	42	4619
16 - 19	1.132 (Double)	61	4865
17 - 20	0.840 (Double)	54	3351
15 - 26	0.030 (Double)	8	3807
26 - 30	0.031	10	7884
30 - 34	0.031	5400	107800
34 - 38	0.031	165	4375
38 - 23	0.060	169	3943
23 - 50	0.060	169	3943
50 - 46	0.031	165	4375
46 - 42	0.031	5400	107800
42 - 26	0.031	10	7884
27 - 31	0.277	10	11105
31 - 35	0.027	169	26705
35 - 39	0.027	85	3641
51 - 47	0.027	85	3641
47 - 43	0.027	169	26705
43 - 27	0.277	10	11105
40 - 25	0.050	36	2602
25 - 52	0.050	36	2602
59 - 60	0.067 (Double)	29	1404
55 - 56	0.020 (Double)	250	24042
56 - 61	0.032 (Double)	47	3245
66 - 62	0.032 (Double)	47	2335
67 - 63	0.070 (Double)	47	3127
1 - 68	0.100 (Double)	31	7626
69 - 64	0.360 (Double)	70	4064

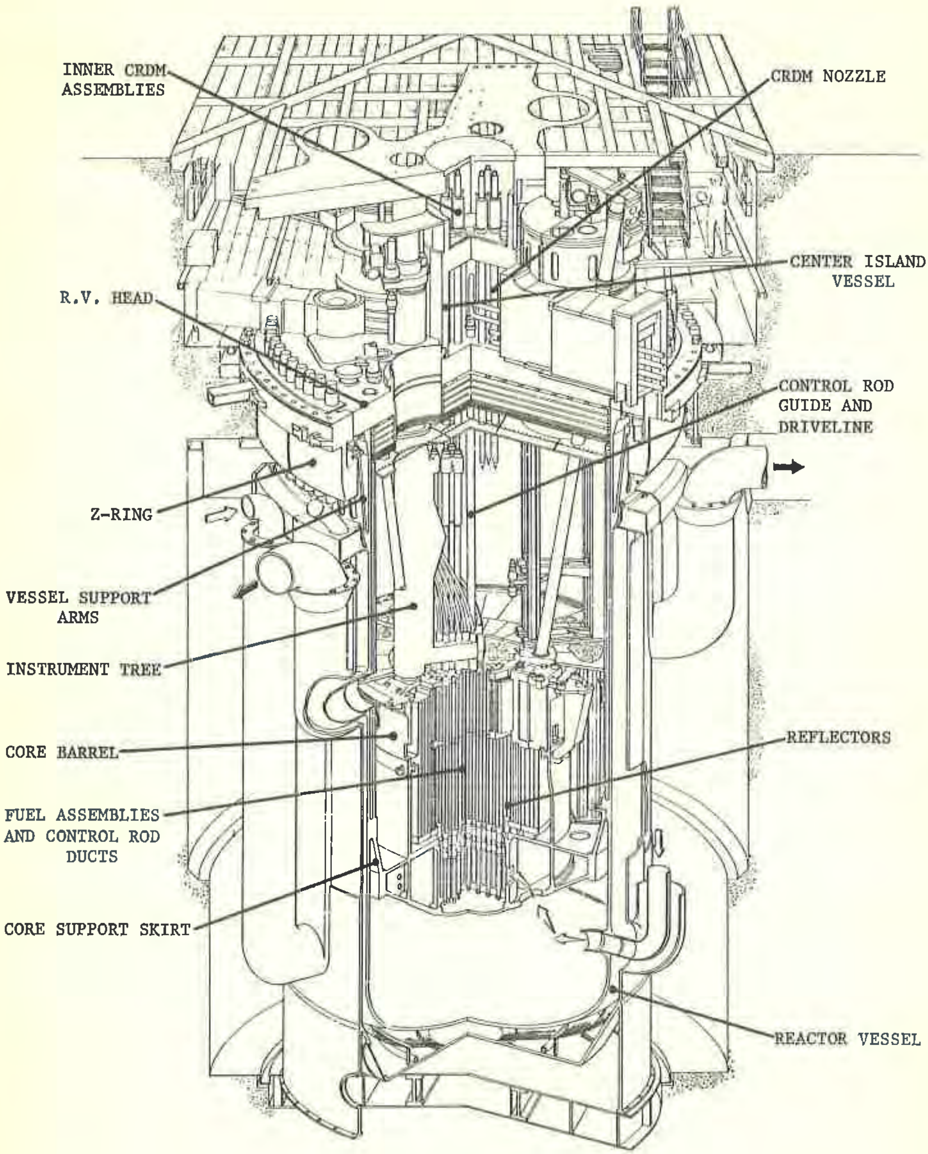

Figure 1 - Liquid Metal Fast Reactor System

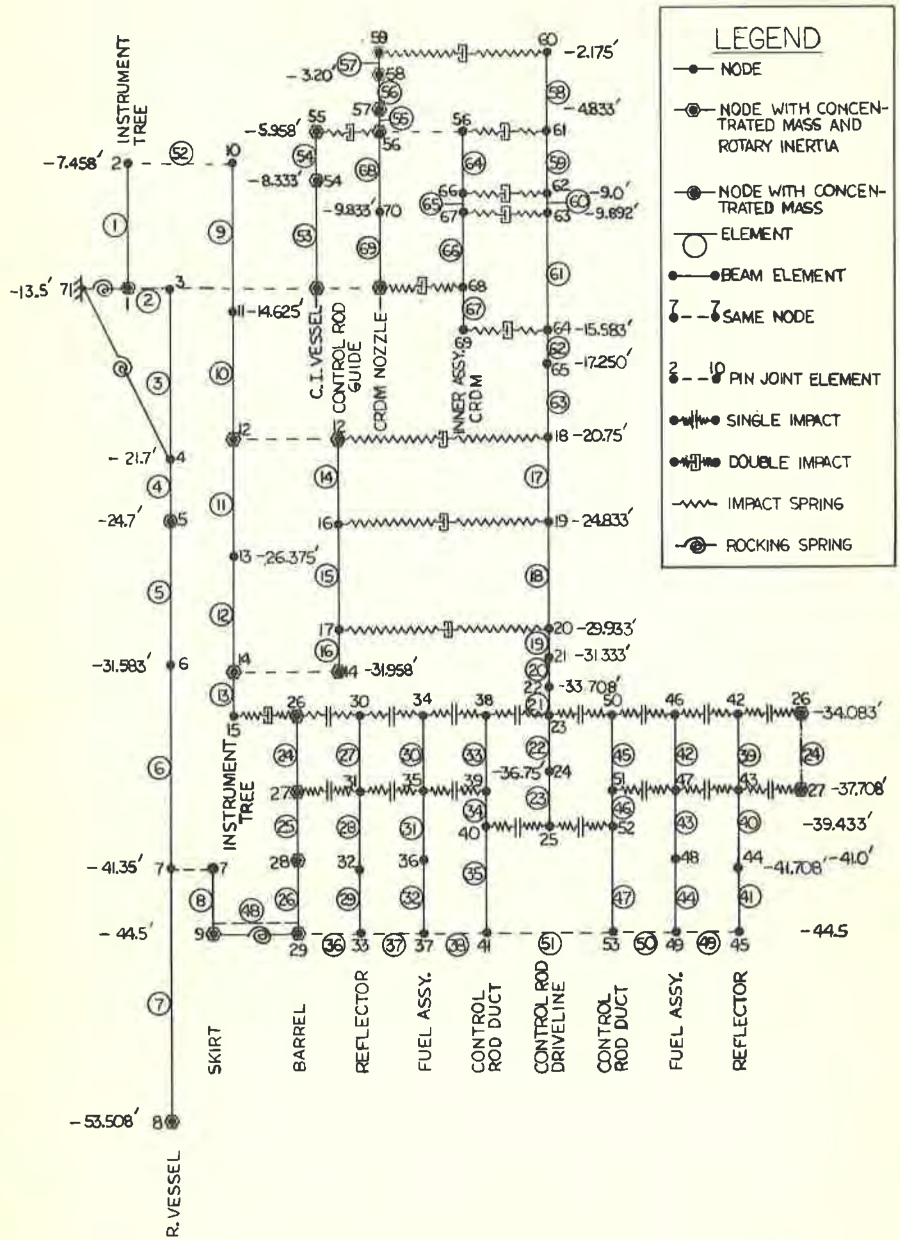

Figure 2 - Mathematical Model for Seismic and Scram Analysis

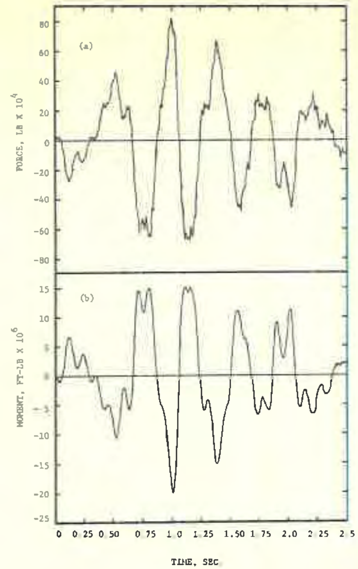

Figure 3 - Seismic Responses at Reactor Vessel Supports; (a) Force; (b) Moment

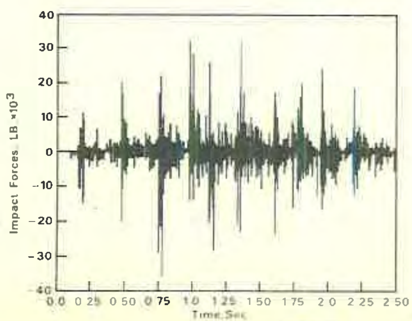

Figure 4 - Total Impact Forces on All Driveline Impact Nodes

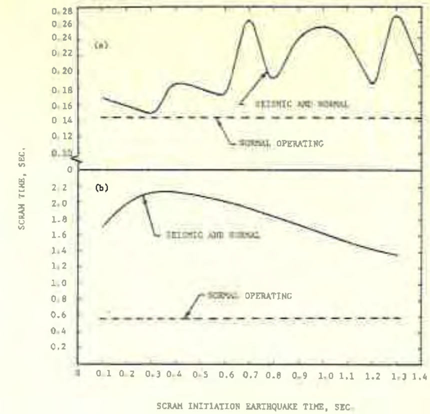

Figure 5 - Scram Time Vs. Scram Initiation Earthquake Time; (a) 5 in. Rod Travel; (b) 27 in. Rod Travel

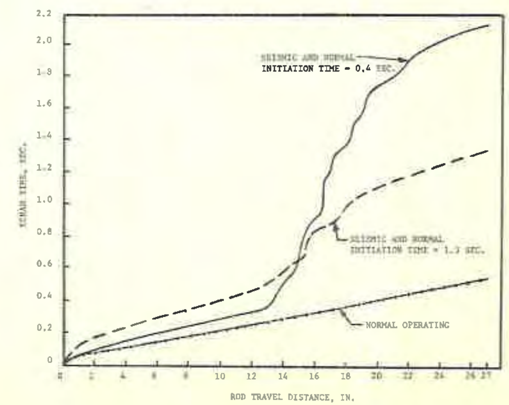

Figure 6 - Scram Time Vs. Rod Travel Distance